Technical Report

Influences of tool shoulder diameter to plate thickness ratio (D/T) on stir zone formation and tensile properties of friction stir welded dissimilar joints of AA6061 aluminum–AZ31B magnesium alloys

S. Malarvizhi *, V. Balasubramanian

Centre for Materials Joining & Research (CEMAJOR), Department of Manufacturing Engineering, Annamalai University, Annamalai Nagar 608 002, Tamil Nadu, India

ABSTRACT

Friction stir welding (FSW) is capable of joining dissimilar materials. In FSW, a rotating shoulder with a profiled pin moves between sheets of the pieces to be joined. As the rotating tool travels along the weld line, frictional heat is generated between the base material and tool shoulder. This heat is however lower than in fusion welding methods. In this work the influences of the tool shoulder diameter (one of the heat generation source) on the macrostructure, microstructure and tensile properties of the dissimilar AA6061 Aluminum and AZ31 Magnesium alloys were experimented. From this investigation, it was found that the joints fabricated using a shoulder diameter of 21 mm (3.5 times the plate thickness) exhibited superior tensile properties compared to its counterparts.

© 2012 Elsevier Ltd. All rights reserved.

1. Introduction

Dissimilar welding of aluminum (Al) and magnesium (Mg) alloys would achieve weight reduction and high efficiency of production by a substitution of Mg alloys for Al alloys. However, fusion welding of Al and Mg alloys always produces coarse grains and large brittle intermetallic compounds in the weld metal region [1,2]. Conventional welding processes such as gas tungsten arc welding (GTAW), laser beam welding (LBW) and electron beam welding (EBW) can be applied to join dissimilar Al and Mg alloys. However, because of high reflectivity of Al and Mg alloys, the energy efficiency of LBW is low. Low melting elements such as Mg and Zn causes evaporation during EBW. High heat exchange ratio cause wider weld bead and coarse grains in GTA welding [3].

Friction stir welding (FSW), a solid state joining process can avoid many problems associated with fusion welding processes, thereby defect free welds having excellent properties can be produced even in some materials with poor fusion weldability [4]. In friction stir welding a rotating shouldered tool with a profiled pin moves along the butt line of the pieces to be joined. As the rotating tool travels along the weld line, frictional heat is generated between the interface of tool and specimen. This heat is, however; significantly lower than in fusion welding methods [5]. In consequence, maximum temperature in the weld seam and the adjacent base material are also lower, which is usually beneficial with

respect to distortion and the residual stress state of the joint. Moreover, because it does not involve melting, FSW has a great potential for joining dissimilar materials such as Al and Mg alloys.

Hirano et al. [6] stated that the good weld was achievable by FSW especially for dissimilar joints with Al, particularly due to the comparatively low amount of intermetallic phase formed as a consequence of the low diffusion rate and reduced amount of chemical reaction compared to fusion welds. This low diffusion rate results from the short dwell time and low process temperatures. Coelho et al. [7] concluded that FSW of Al alloys to Mg alloys is feasible and joints with good mechanical properties can be obtained. Mofid et al. [8] reported that the formation of intermetallic compounds in the stir zone of dissimilar Al–Mg friction stir welds affects the mechanical properties of the joint significantly. However, many details of microstructure evolution in FSW of Al alloys to Mg alloys are not yet fully understood. This is particularly so in regard to intermetallic layer formation with respect to the process and tool parameters used.

In FSW, the non-consumable tool plays a vital role in generating heat by means of friction to plasticize the materials to be welded. Though the tool has three different portions such pin, shoulder and shank, the pin diameter and shoulder diameter decide the quantinum of heat generated during FSW. Of the two, shoulder diameter is considered to be the primary heat generation source since the contact area between shoulder surface and the butted materials top surface is higher than the other contacting areas.

In FSW of similar materials (Al to Al alloys; Mg to Mg alloys), as a thumb rule, the tool shoulder diameter (D) is generally kept as 3 times the plate thickness of the materials to be welded. However, this ratio may not be correct while friction stir welding of

* Corresponding author. Tel.: +91 4144 239734 (O); fax: +91 4144 238080/238275.
E-mail addresses: jeejoo@rediffmail.com (S. Malarvizhi), visvabalu@yahoo.com, balasubramanian.v2784@annamalaiuniversity.ac.in (V. Balasubramanian).

dissimilar materials such as Al and Mg alloys (due to the difference in crystal structure and related plastic flow behavior). Hence, in this investigation, an attempt was made to study the effect of tool shoulder diameter (in terms of plate thickness (T) of the materials to be joined) on stir zone formation and subsequent tensile properties of dissimilar joints of AA6061 Al and AZ31B Mg alloys.

2. Experimental details

Rolled plates of (200 mm × 150 mm × 6 mm) Al and Mg alloys were placed at retreating and advancing sides of the rotating tool respectively as shown in Fig. 1. The chemical composition and mechanical properties of base metals are presented in Tables 1 and 2, respectively. All the joints were butt welded and were carried out using tools made of high speed steel. The shoulder diameter of the tool was varied from 12 to 24 mm (2–4 times the plate thickness) and the fabricated tools are displayed in Fig. 2; the probe had a diameter of 6 mm and a height of 5.7 mm. The tool was fed at a constant traverse rate into the joint of the two plates to be welded. The welding parameters and tool details are presented in Tables 3 and 4 respectively. The photographs of fabricated joints are displayed in Fig. 3. Heat input was calculated using the following equation proposed by Heurtier et al. [9].

$$q = \frac{2\pi}{3S} \times \mu \times P \times \omega \times R_s \times \eta \tag{1}$$

where q – specific heat input in kJ/mm; μ – coefficient of friction; P – axial force in kN; ω – angular velocity in rps; and η – process efficiency.

The specimens for metallography were cut perpendicular to the welding direction using wire cut electrical discharge machine. All the weld samples were polished using a grit sequence of 220, 320, 500, 800 and 1200 as specified in ASTM E407-09 guidelines [10]. The effect of water on the Mg side of the welds was minimized by constant cleaning with ethyl alcohol. These samples were further polished using a polishing cloth and polishing solutions of 1, 0.3 and 0.05 Am alumina in a solution of 75% ethanol and 25% glycerol. Again, the ethanol base was used to minimize contamination of the Mg samples. The Mg–Al samples were pre-etched with a solution of 2 g NaOH in 100 ml distilled water, and subsequently rinsed in a solution of 5 ml HNO$_3$ in 95 ml distilled water. This

Table 1
Chemical composition (wt.%) of base metals.

Alloy	Al	Mn	Zn	Ni	Si	Fe	Cu	Cr	Mg
AZ31B-O	3.0	0.3	0.9	0.002	0.20	0.003	0.002	–	Bal
AA6061-T$_6$	Bal	0.15	0.25	–	0.6	0.75	0.20	0.04	1.2

served to bring out the lamellar-like shear bands and other fine microstructures from the intercalated weld zone prior to the application of the dedicated etchants. A picral etchant was employed to etch the Mg side of the welds in all samples. The picral etch is a solution of 14 ml picric acid, 2 ml glacial acetic acid and 2 ml distilled water. The picric acid solution contained 2 g picric acid in 20 ml ethanol (this ratio was maintained in all cases). Cotton swabs and/or cotton buds were used for applying this etchant onto the Mg alloy. A variation of the Keller's reagent, with equal parts methanol, HF and HNO$_3$, was used to etch the Al in the Mg–Al samples. The Al side of the weld was swabbed multiple times (cleaned with ethanol after a few seconds of swabbing) until visible etching was obtained. The etched samples were viewed using light optical microscopy. The overall weld cross section was analyzed at low magnifications to view the entire span of the weld zone, showing the base materials, the transition zones and the stir zone. The weld zone was further analyzed at higher magnifications to view the intercalated microstructures. Un-notched smooth tensile specimens were prepared to evaluate the transverse tensile properties of the joints such as yield strength, tensile strength and elongation. Tensile testing was carried out using 100 kN, electromechanical controlled universal testing machine (Fie-Blue Star, India; model Unitek-94100). ASTM E8 M-04 guidelines [11] were followed for preparing and testing the tensile specimens.

3. Results

3.1. Macrostructure

Top surface of the welded joints (beads) are free from visible defects Fig. 3. However, the weld cross section at low magnification shows defects such as tunnel defect, piping defects, and pin holes. The effect of tool shoulder diameter on macrostructure of the weld cross section was illustrated in Table 5. Of the five joints fabricated,
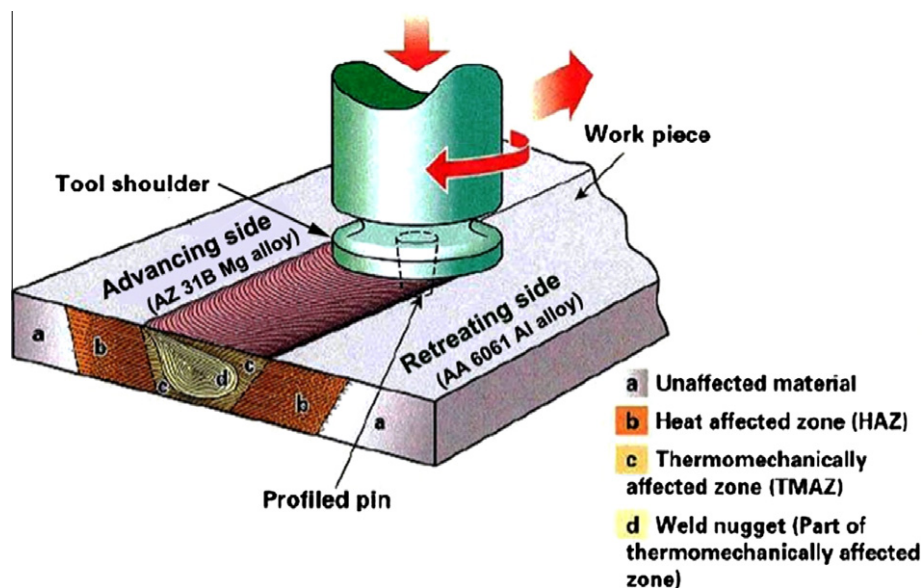

Fig. 1. Schematic of FSW.

Table 2
Mechanical properties of base metals.

Alloy	Yield strength (MPa)	Tensile strength (MPa)	Elongation in 50 mm gauge length (%)	Hardness @ 15 s (HV$_{0.05}$)
AZ31B-O[a]	175	216	15	80
AA6061-T$_6$[b]	280	311	20	105

[a] O – Annealed condition.
[b] T$_6$ – Solution heat treated and then artificially aged.

Fig. 2. Tools with different shoulder diameters used to fabricate the joints.

Table 3
FSW process parameters used to fabricate the joints.

Tool rotational speed (rpm)	400
Welding speed (mm/s)	0.33
Axial force (kN)	12

Table 4
FSW tool details.

Tool material	HSS
Shoulder diameter (mm)	12, 15, 18, 21, 24
Tool pin profile	Tapered pin
Pin diameter (major) (mm)	6 mm
Pin diameter (minor) (mm)	5 mm
Pin length (mm)	5.7
Tool inclination	0˚

the joint fabricated using a shoulder diameter of 21 mm yielded defect free joint. This may be one of the reasons for higher tensile strength of the joint fabricated using a tool with 21 mm shoulder diameter.

3.2. Microstructure

The cross section of the defect free weld joint alone analyzed using optical microscopy. The base material microstructure of AA6061 and AZ 31B consists of grains of unequal size and distribution as shown in Fig. 4. Fig. 5a shows the microstructure in the shoulder influenced region between the Al alloy base material and the stir zone. The grain size can be clearly seen to decrease as it transitions from the base material. There is then a sharp demarcation where it passes into the stir zone. The grain size in the 6061-T6 material away from the transition zone is shown in

Fig. 5b. No appreciable grain growth can be detected in this case. Optical micrographs show the Mg side had recrystallized grains from the transition zone along with the intercalated flow patterns. Prominent grain growth is also observed in the dynamically recrystallized Mg alloy in the transition region (Fig. 5b). The recrystallized Mg grains in the transition zone can be seen to be fine, homogeneous and equiaxed. The frictional heat created by the rubbing of the tool shoulder and the mechanical stirring of the materials by the tool probe. Hence the weld zone produces DRX of both the material. Similar observations were made by other investigators [12,13]. Due to this severe plastic deformation in the weld zone, there is flow of material in the solid state and also mixed flow pattern of both the material were observed in Fig. 5c.

In comparison with the microstructures of in the gas tungsten arc welded dissimilar joints of the Mg–Al were the weld metal is composed of columnar crystals which grow into the weld metal and also some dendrite crystals [14]. Here, DRX facilitates the solid-state flow that enables FSW. The adiabatic heat arising from the deformation-induced DRX that contributes to the weld zone temperatures reaching approximately 0.8 TM (TM is the melting point of the material) which in turn also shows the weld zone intercalated microstructures, with lamellar-like shear bands rich either in Al or Mg [15]. The lamellar-like shear bands have been seen previously in other work on dissimilar FSW welds [16]. The microstructure Fig. 5d shows complex intercalated flow patterns, in which recrystallized Mg and Al alloys are swirled together to form a complex mesh, as seen in other dissimilar FSW work [17] also comprises microstructures from the 6061-T6 side of the weld.

3.3. Tensile properties

The specimens were tensile tested and transverse tensile properties such as yield strength, tensile strength and percentage of
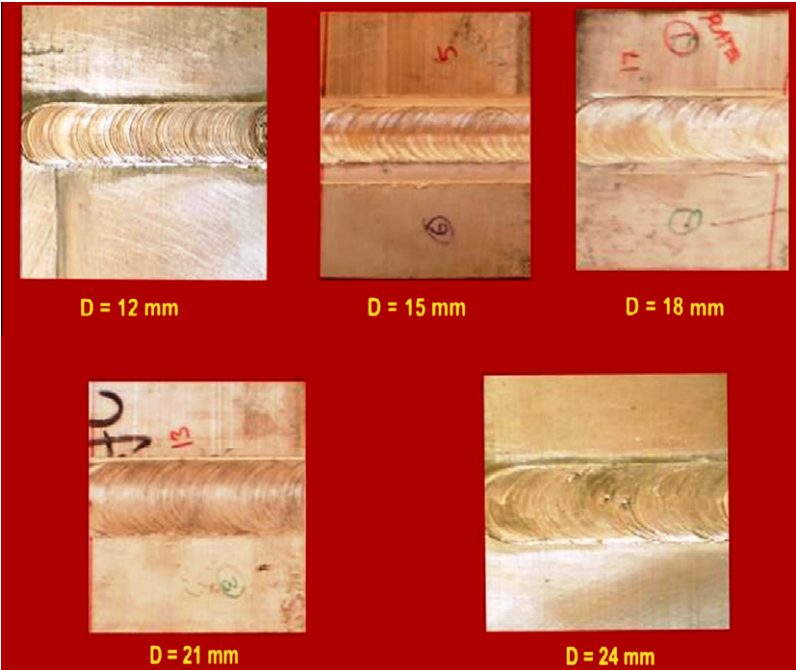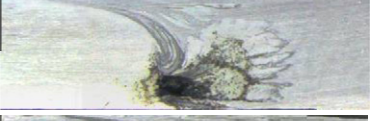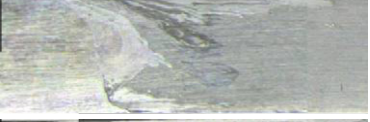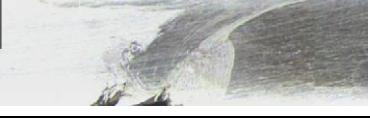
Fig. 3. Fabricated joints.

Table 5
Effect of tool shoulder diameter on macrostructure.

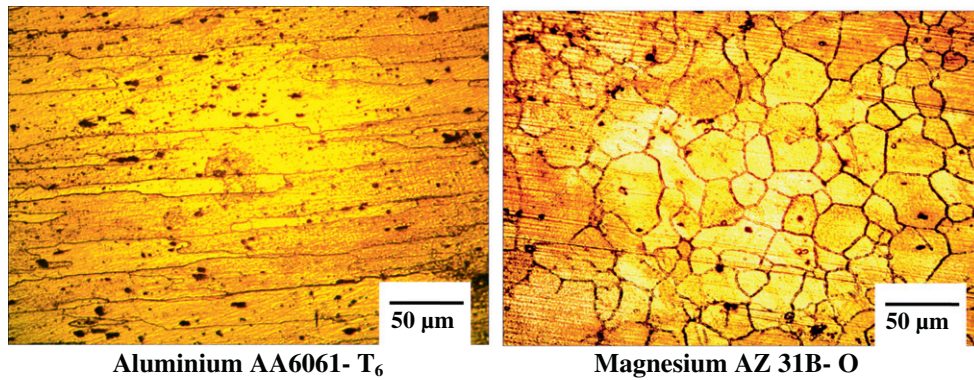| Tool shoulder diameter (mm)	D/T	Top surface of the welded joint	Macrostructure of the joint cross section		Observations
			AS	RS	
12	2				Tunnel defect at the advancing side
15	2.5				Tunnel defect at the retreating side
18	3				Tunnel defect at the advancing side
21	3.5				No defect
24	4				Tunnel defect at the root

elongation of the joints were evaluated. The dimension of tensile specimen is presented in Fig. 6. The specimen before and after tensile testing are displayed in Fig. 7. In each condition, three specimens were tested and the average of three results is presented in Fig. 8. Of the five joints, the joint fabricated using a tool with shoulder diameter of 21 mm (3.5 times the plate thickness) yielded better tensile properties. The tensile strength exhibited by this joint is 192 MPa which is approximately 62% of the tensile strength of the

AA6061 aluminum alloy and 88% of the tensile strength of AZ31B magnesium alloy.
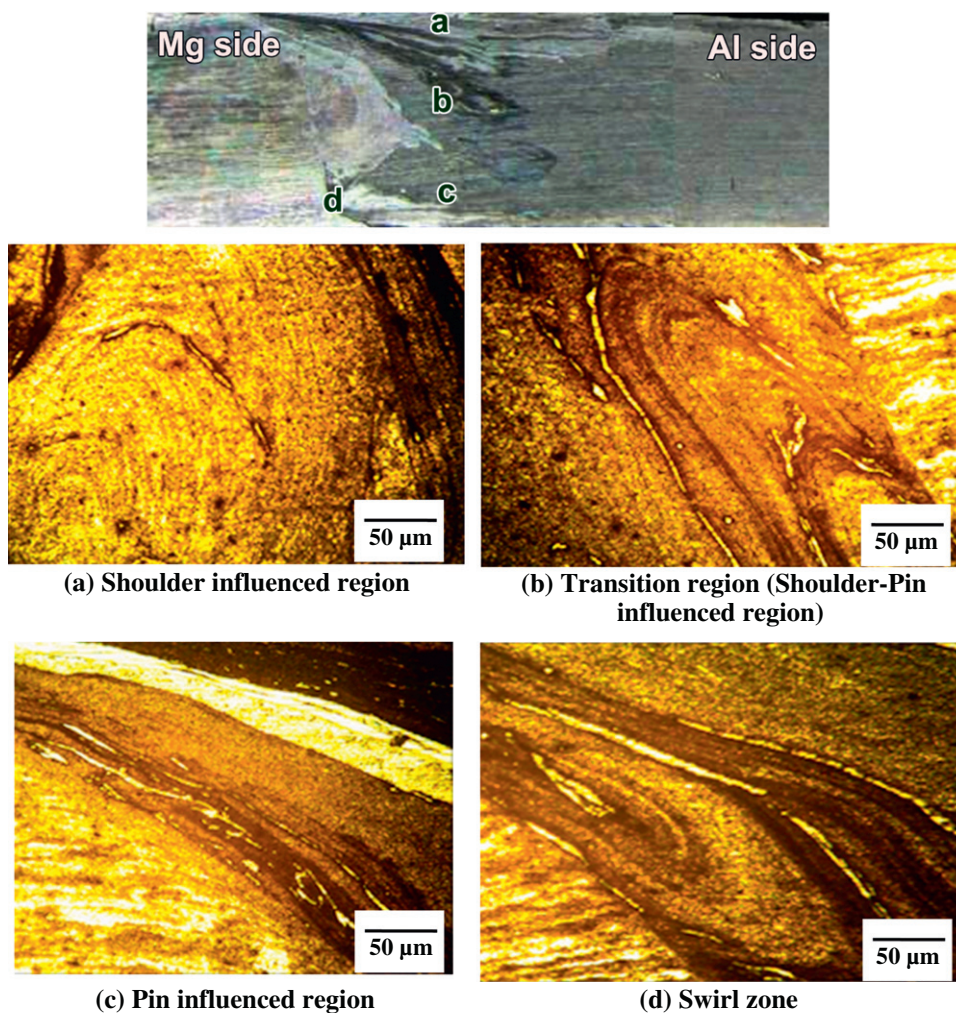
3.4. Lowest hardness distribution profile (LHDP)

In welded joints, the failure will occur along the weakest region (lowest hardness region). Normally, the hardness profile was measured either along the mid thickness of welded plate or along the

Aluminium AA6061- T₆   **Magnesium AZ 31B- O**

Fig. 4. Optical micrograph of base metals.

(a) Shoulder influenced region

(b) Transition region (Shoulder-Pin influenced region)

(c) Pin influenced region

(d) Swirl zone

Fig. 5. Microstructure of various region of dissimilar aluminum (AA6061)–magnesium (AZ31B) alloy joint.

top, center and bottom of the plate thickness to determine the lowest hardness points [18]. However it should be pointed out that such hardness profiles could not predict the fracture behavior of welded joints because of limited hardness points. Recent studies [19] revealed that the construction of the hardness distribution profile around HAZ throughout the whole thickness of friction stir welded AA6061 aluminum alloy. It is indicated that the fracture paths of joint was consistent with the lowest hardness distribution.

In this study, the hardness distribution maps were constructed by measuring the Vickers microhardness at an interval of 0.5 mm along the cross section of FSW joint fabricated using a tool with 21 mm shoulder diameter and presented in Fig. 9a. The fracture path of FSW joints is consistent with the lowest hardness distribution profile and the fracture location is illustrated in Fig. 9b. The failure of FSW joint was observed at advancing side where the lowest hardness was recorded.
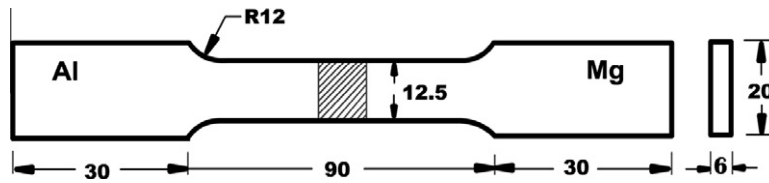
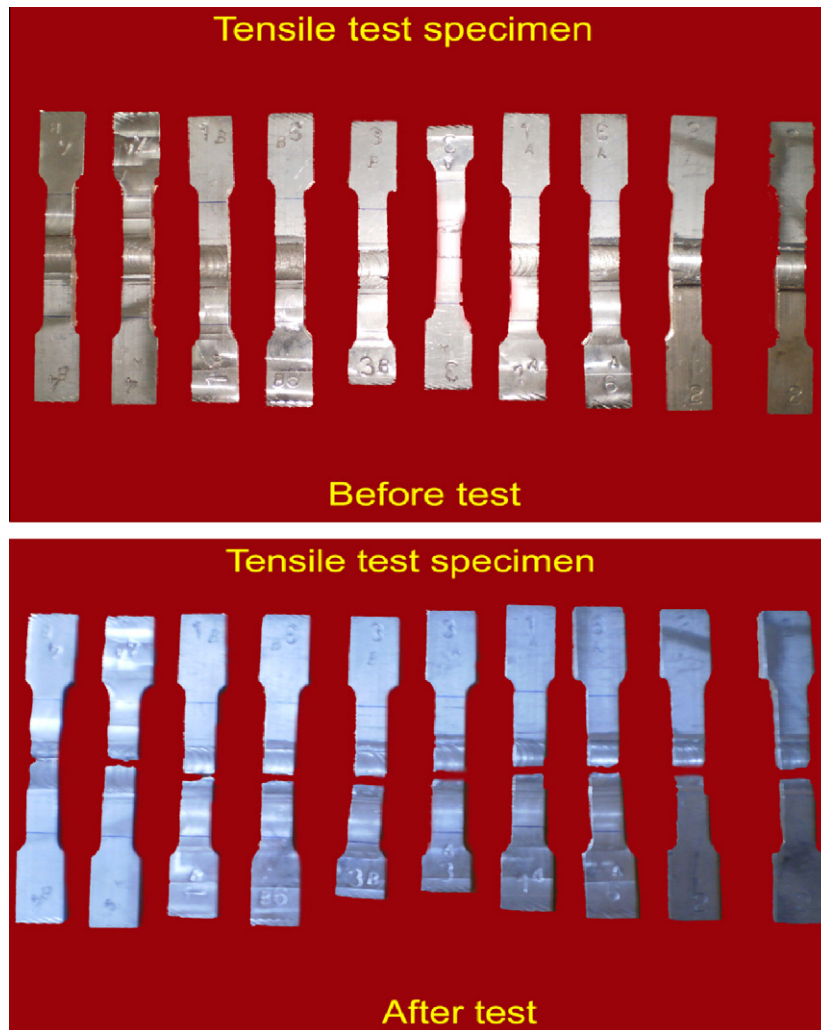**Fig. 6.** Dimension of tensile specimen used.


Fig. 7. Tensile specimen before and after test.

4. Discussion

Colligan [20] investigated the material flow behavior of aluminum alloys during FSW and he opined that two effects are responsible for the creation of the material flow in the stir zone. First is the extrusion process, where the applied forces and the motion of the tool pin propel the material after it has undergone the plastic deformation. The second is due to the rotation of the pin that serves as the driving force for the flow. Due to high values of viscosity, the stirring effect is much more distinct in comparison to the extrusion driven flow. Ouyang et al. [21] visualized material flow behavior during FSW of similar and dissimilar aluminum alloys and they found that in friction stir welds not all material influenced by the pin is actually "stirred" in the welding process. Much of the material movement takes place by simple extrusion. Modest vertical flow and material extrusion from front to back around both sides of the pin is possible and the role of the rotating pin is to provide frictional heating to make the extrusion possible. Ying et al. [22] have studied the solid state flow visualization of FSW of AA2024 and AA6013 aluminum alloys and they observed that the flow of the plate material on the advancing side and the retreating side are different. The material on the retreating side never enters into the rotational zone near the pin, but the material on the advancing side forms the fluidized bed near the pin and rotates around it. After several revolutions the material on the advancing side starts to slough off in the wake behind the pin. In
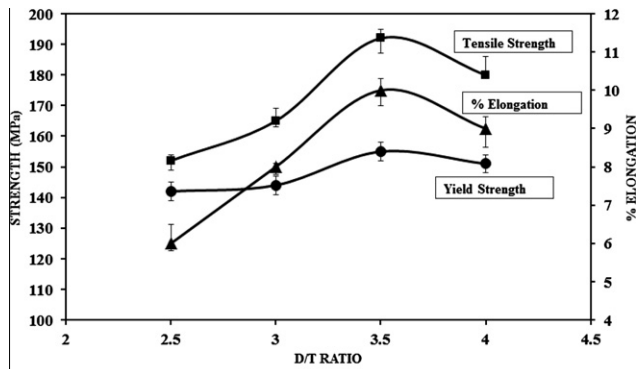
(a) Effect of D/T ratio on Tensile properties
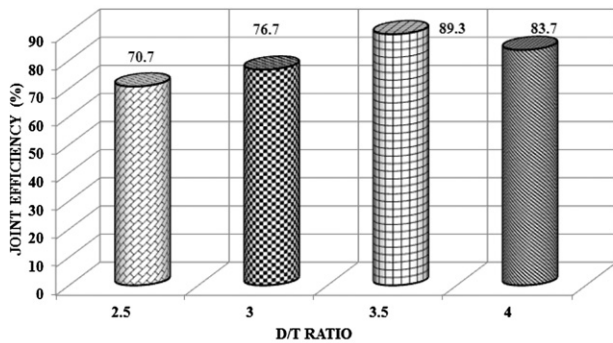
(b) Effect on D/T ratio on Joint Efficiency

Fig. 8. Effect of shoulder diameter on tensile properties.

the stir zone the grain structure is characteristic of the idealized fluid particle concept which accommodates shear flow in liquid and liquid-like regimes.

It is well known that a typical stir zone of FSW joint contains five different regions: (i) Shoulder influenced region (flow arm) near the top surface of the plate. (ii) Shoulder-pin (transition region) near the mid thickness of the plate. (iii) Pin influenced region-near the bottom surface of the plate. (iv) Vortex region-beneath the pin. (v) Swirl zone within the pin influenced region but in the advanced side. The formation of defect free stir zone with the above said sub regions is mainly dependent on the flow behavior of the materials under pin driven extrusion and shoulder driven forging action [23].

Since FSW is a hot working process, the temperature required for welding must reach well above the recrystallization temperature of the materials to be joined so as to derive the benefits of dynamic recrystallization in the stir zone. The material will attain the required temperature only when the welding conditions and the parameters are selected properly during FSW [24]. Under these circumstances, tool shoulder diameter plays a vital role since it is considered to be the primary source of heat generation. It can also be understood from Eq. (1), the tool shoulder radius is having directly proportional relationship with the frictional heat generation

In this investigation, five joints were fabricated using five tools (with varying shoulder diameter and constant pin profile). Of the five joints, the joint fabricated using a tool with the shoulder diameter of 21 mm (3.5 times plate thickness) yielded higher tensile strength and this is mainly due to the formation of defect free stir zone. The joints fabricated by all other tools yielded lower tensile strength due to the presence of defect in stir zone and it is evident from macro structure analysis (Table 5).

In all the joints, macro level defects are not visible in shoulder influenced region and shoulder-pin influenced region. But the pin influenced region, especially the swirl zone, contains some form of defects. The joint fabricated by a tool with shoulder diameter of 12 mm, contains a huge tunnel defect in the advancing side of pin influenced region. Similarly, the joint fabricated by a tool with shoulder diameter of 15 mm also contains a tunnel defect at the same location but smaller in size. The joint fabricated by a tool with the shoulder diameter of 18 mm also contains a tunnel defect at the same location but much smaller in size. This suggest that increasing the tool shoulder diameter from 12 mm to 18 mm (2T to 3T) reduces the size of the defect at swirl zone and tool shoulder diameter of 21 mm completely eliminated the formation of defect

← Distance from the weld centre (in mm)															W
-21	-19	-17	-15	-13	-11	-9	-7	-6	-5	-4	-3	-2	-1	0	E L D
86.4	83.2	79.8	78.2	82.3	80.9	91.2	86.4	79.8	76.4	81.5	83.6	86.7	85.3	81.2	
93.2	88.6	74.7	85.1	83.3	94.3	77.3	74.6	73.0	89.3	76.8	81.3	90.3	86.5	84.3	C E
87.7	73.4	84.8	85.9	94.3	90.6	85.7	73.2	97.6	86.0	92.0	81.7	96.3	109	79.9	N T
85.6	83.1	80.8	79.7	86.1	85.2	76.7	116	86.8	77.8	79.2	85.8	79.0	99.0	96.3	R E
81.2	76.9	66.7	74.4	76.9	68.9	61.1	68.5	76.5	71.5	68.5	70.9	73.2	76.1	69.9	

Fig. 9a. Lowest hardness distribution profile (LHDP).
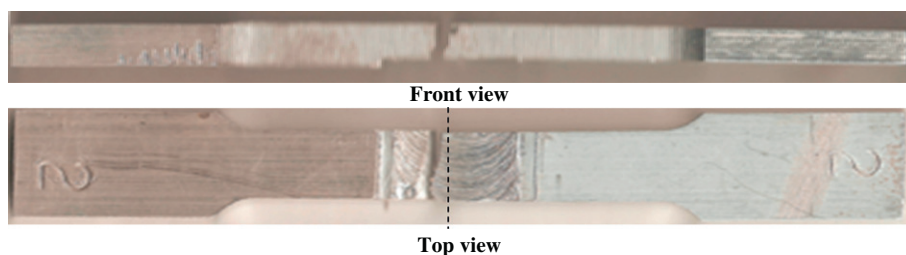

Front view

Top view

Fig. 9b. Fracture location of tensile specimens.

at swirl zone. This indicates that the minimum heat input required to avoid defects in swirl zone (which is more vulnerable for defect) should be in range of 1.2–1.3 kJ/mm. If the heat input is lower or higher than this value, then it leads to defect formation in the swirl zone.

Since the swirl zone is within the pin influenced region, the effect of tool shoulder on the formation of defects in swirl zone is minimal. However, as mentioned earlier, the shoulder driven material (by the forging action) and pin driven material (by extrusion action) are mixed at advancing side (swirl zone) and then transported to retreating side. The material mixing (Al and Mg alloys) at the swirl zone produces intercalated microstructure (alternate layers of Al and Mg alloys) in dissimilar welding (Fig. 5d). Insufficient material flow at low heat input conditions and excess material flow at high heat input conditions will lead to improper mixing of material at swirl zone subsequently resulted in some type of defects.

In FSW of similar materials the tool shoulder is normally kept as three times the plate thickness and it is proved by many investigations [12,13]. However, the FSW of dissimilar materials, especially for Al to Mg combinations, the heat input required is marginally higher to enable the proper material mixing and hence the optimum shoulder diameter must be 3.5 times the thickness of the plate to be joined.

5. Conclusions

In this investigation, the tensile properties of dissimilar magnesium (AZ31B)–aluminum (AA6061) joints were evaluated. Of the five joints fabricated using tools with different shoulder diameters, the joint fabricated with a tool shoulder diameter of 21 mm (3.5 times the plate thickness) yielded maximum tensile strength of 192 MPa and the joint efficiency is 89% compared with the lower strength base metal.

Dynamic recrystallization was enabled by the frictional heat from the tool shoulder and tool nib, heat generated by mechanical stirring of the materials by the nib, mostly adiabatic heat contributing to DRX through deformation due to the optimum tool shoulder diameter. Complex intercalated microstructures in the weld zone, with swirls and vortices indicative of the flow pattern of the dissimilar metals. Complex intercalated microstructures in the FSW zone contribute to elevated hardness readings in the weld zone.

Acknowledgment

References

[1] Liu Peng, Li Yajiang, Geng Haoran, Wang Juan. Microstructure characteristics in TIG welded joint of Mg/Al dissimilar materials. Mater Lett 2007;61:1288–91.
[2] Shang J, Wang K, Zhou Q, Zhang D, Huang J, Li G. Microstructure characteristics and mechanical properties of cold metal transfer welding Mg/Al dissimilar metals. Mater Des 2012;34:559–65.
[3] Kwon YJ, Shigematsub I, Saito N. Dissimilar friction stir welding between magnesium and aluminum alloys. Mater Lett 2008;62:3827–9.
[4] Thomas WM, Nicholas ED, Needham JC, Murch MG, Templesmith P, Dawes CJ. Friction stir welding butt welding. US5460317; 1995.
[5] Yutaka Sato S, Seung Hwan Park C, Masato Michiuchi, Hiroyuki Kokawa. Constitutional liquations during dissimilar friction stir welding of Al and Mg alloys. Scripta Mater 2004;50:1233–6.
[6] Hirano S, Okamoto K, Doi M, Okamura H, Inagaki M, Aono Y. Microstructures of the interface in magnesium alloy to aluminum alloy dissimilar joints produced by friction stir welding. Weld Int 2004;18:702–8.
[7] Coelho RS, kostka A, Sheiki S, Dos Santos J, Pyzalla AR. Microstructure and residual stress formation in an AA6040 to AZ31B friction stir welds. Adv Eng Mater 2008;10:961.
[8] Mofid MA, Abdollah-zadeh A, Malek Ghaini F. The effect of water cooling during dissimilar friction stir welding of Al alloy to Mg alloy. Mater Des 2012;36:161–7.
[9] Heurtier P, Jones MJ, Desrayaud C, Driver JH, Montheillet F, Allehaux D. Mechanical and thermal modelling of friction stir welding. J Mater Process Technol 2006;171:348–57.
[10] ASTM E 407–09. Standard practice for microetching Metals and alloys. ASTM International; 2009.
[11] ASTM International Standard E8M–06. Standard test methods for tension testing of metallic materials. ASTM, International; 2006.
[12] Somasekharan AC, Murr LE. Characterization of complex, solid-state flow and mixing in the friction-stir welding (FSW) of aluminum alloy 6061–T6 to magnesium alloy AZ91D using color metallography. J Mater Sci 2006;41:5365–70.
[13] Zettler R, da Silva AAM, Rodrigues S, Blanco A, dos Santos JF. Dissimilar Al to Mg alloy friction stir welds. Adv Eng Mater 2006;8:415–21.
[14] Yasui T, Shimoda Y, Tsubaki M, Fukumoto M. In: Proc Int Offshore Polar Eng Conf, Korea; 2005. p. 39.
[15] Anand Somasekharan C, Lawrence Murr E. Fundamental studies of the friction-stir welding of magnesium alloys to 6061–T6 aluminum. Magnesium Technol 2004:31–6.
[16] Flores RD, Murr LE, Shindo D, Trillo EA. Friction-stir welding of metals and alloys: fundamental studies of solid-state and intercalated flow. Int Conf Proc Manuf Adv Mater 2000.
[17] Murr LE, Li Y, Trillo EA, Flores RD, McClure JC. Microstructures in friction stir welded metals. J Mater Process Manuf Sci 1998;7:145–61.
[18] Mishra RS, Ma ZY. Friction stirr welding and processing. Mater Sci Eng [A] 2005;50:1–78.
[19] Ren SR, Ma ZY, Chen LQ. Effect of welding parameters on tensile properties and fracture behavior of friction stir welded Al–Mg–Si alloy. Scripta Mater 2007;56:69–72.
[20] Colligan K. Material flow behaviour during friction stir welding of aluminium. Weld J 1999:229–37.
[21] Ouyang JH, Jandric D, Kovacevic R, Song M, Valant M. Visualization of material flow during friction stir welding (FSW) of the same and dissimilar aluminum alloys. Proc 6th Int Trends Weld Res 2002:229–40.
[22] Ying Li, Murr LE, McClure JC. Solid state flow visualization in the friction stir welding of 2024A1 to 6061Al. Scripta Mater 1999;40(9):1041–6.
[23] Lima EBF, Wegener J, Dalle Donne, Goerigk G, Wroblewski T, Buslaps T, et al. Dependence of the microstructure, residual stresses and texture of AA6013 friction stir welds on the welding processes. Metallkunde 2003;94:908–15.
[24] Oosterkamp A, Djapic Oosterkamp L, Nordeide A. Kissing bond phenomena in solid state welds of aluminum alloys. Weld J 2004:225–31.